

AFM Lithography with a Current-controlled Exposure System

M. Ishibashi, S. Heike, H. Kajiyama, Y. Wada and T. Hashizume

Advanced Research Laboratory, Hitachi, Ltd., Hatoyama, Saitama 350-0395, Japan
Phone: +81-492-96-6111, Fax: +81-492-96-6006, e-mail: isibasi@harl.hitachi.co.jp

(Received: 15 January 1998; accepted: 3 March 1998)

Abstract

An atomic force microscopy (AFM) lithography system using a current-controlled exposure system is developed. We fabricate line-and-space patterns on a commercial negative-type resist, RD2100N (Hitachi Chemical Co.), and evaluate the lithography's characteristics, including the current-voltage (I-V) characteristics, sensitivity curve, cross-sectional shape, dose-margin, resolution, and proximity effect. We find that the cross-sectional shape of the developed resist pattern depends on the exposure dose. The sensitivity, dose-margin, and resolution depend on the resist thickness and a minimum line width of 27 nm is obtained for a 15-nm-thick resist. The proximity effect is much smaller than that of electron beam (EB) lithography. We also evaluate the electric-field mapping inside the resist and explain the characteristics of the AFM exposure system based on the proposed exposure mechanism.

Scanning-probe lithography (SPL) based on scanning tunneling microscopy (STM), atomic force microscopy (AFM), or some other scanning-probe method, is a powerful tool for fabricating nanoscale structures. Ever since the STM-based electron exposure of a Langmuir-Blodgett (LB) film was first demonstrated,[1] STM and AFM have been used for electron exposure of several kinds of resists and sub-100-nm resolution has been successfully obtained. [2-8] However, the characteristics required to perform the lithography have not been investigated in detail. In this paper, we report on the superior characteristics of AFM-based lithography using a current-controlled exposure system.

A commercial contact-mode AFM system was used to control the tip position. A tip with a cantilever was coated with Ti by dc sputter deposition and the radius of the tip apex was inspected using scanning electron microscopy (SEM). The experimental setup was similar to that used in an earlier work[4] except for a second feedback system for adjusting the negative bias voltage applied to the metal-coated tip to control the field emission current constant.[8] The constant current feedback system reduces variation in the width of the line patterns compared with the constant bias feedback system. These results show that the exposure dose is kept constant by using constant current feedback system, even though the resist-thickness is not uniform or the tip shape is changed.

The RD2100N negative resist (Hitachi Chemical Co.), which is a high-resolution EB

resist, was spin-coated onto Si wafer substrates and pre-baked on a hot plate at 75°C for 7 min. To expose the resist with an electron flux from the tip, the tip-to-substrate bias was varied between -10 to -100 V to maintain a constant current of typically 10 pA. Patterns were exposed with a line dose of 0.3 to 110 nC/cm at an AFM scanning speed of 10 to 100 μ m/s. An aqueous-base developer (35% dilution of NMD-W 2.38% obtained from Tokyo Ohka Kogyo) was used as a developer solution. After development, the resist pattern was observed using SEM.

Figure 1 shows the I-V characteristics of the resists using the current-controlled exposure system for resist thicknesses of 15, 40, and 100 nm. To understand the conduction mechanism in the resist film, we analyzed the I-V characteristics based on Fowler-Nordheim conduction. We found that Fowler-Nordheim

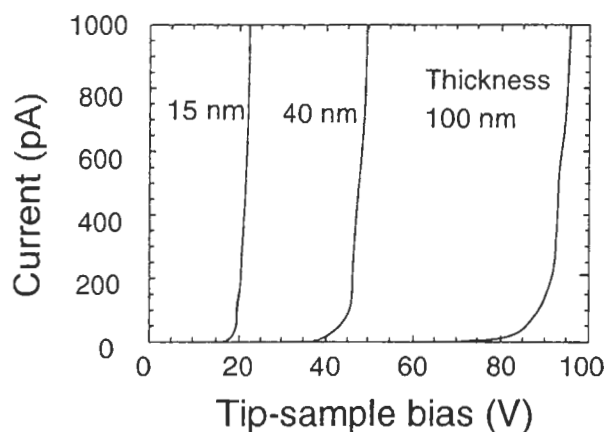


Fig.1 Current-voltage characteristics for resist thicknesses of 15, 40, and 100 nm.

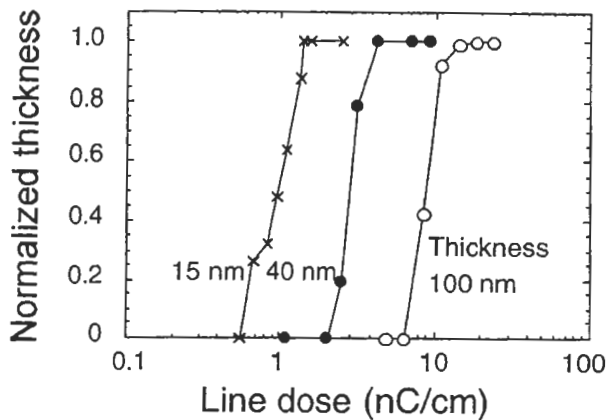


Fig.2 Sensitivity curves of the resist for resist thicknesses of 15, 40, and 100 nm.

conduction (field emission) explains most of the I-V characteristics and the obtained work function, 2.4 eV, is reasonable. However, ionic conduction, Poole-Frenkel conduction, and Schottky conduction cannot be ruled out based on only the I-V curve fitting. Several mechanisms may be at work.

The sensitivity curves of the resists for thicknesses of 15, 40, and 100 nm are shown in Fig. 2. The normalized thickness for each line dose is defined as the ratio of the thickness of the line pattern after and before development. The sensitivity, defined as the line dose for one-half of the normalized thickness, was 1.0, 2.9, and 8.8 nC/cm, respectively, for the resist thicknesses of 15, 40, and 100 nm. The bias voltages that give these sensitivity points are respectively 11, 34, and 79 V, and the electric field averaged over the resist thickness was approximated as 8 MV/cm for all the cases. Thus, the results imply that the cross-section of an electron for the chemical reaction in the resist does not depend on the bias voltage. The (value, which shows the steepness of the sensitivity curve, was 3, 6, and 4 for the resist thicknesses of 15, 40, and 100 nm.

Figure 3 shows cross-sectional SEM micrographs of the developed line patterns for the resist thickness of 100 nm. The resist profiles are steep, although the top of the resist is deformed. An AFM image of the resist surface after pattern exposure shows that the resist surface was deformed even before development. The depth of the indentation was measured to be approximately 10 nm, which is 10% of the resist thickness. These results indicate that the indentation made by the tip

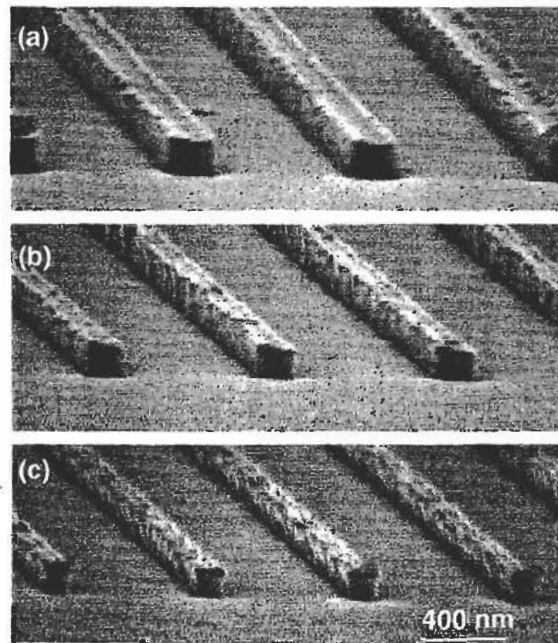


Fig.3 Cross-sectional SEM photographs of the developed line resist patterns for the line dose of (a) 105, (b) 28, and (c) 13 nC/cm.

into the surface of the resist was due to the strong Coulomb force supplied from the bias voltage between the tip and the substrate. It can also be seen from Fig. 3 that the cross-sectional shape of the resist is trapezoidal (narrow top and wide bottom) for a large exposure dose and upside-down trapezoidal (wide top and narrow bottom) for a small exposure. The ability to control the resist shape by changing the exposure dose is another important feature of this system.

The electric field in the resist region was calculated in order to discuss the exposure mechanism and the cross-sectional shape of the resist in more detail. We assumed that the tip was spherical and used a typical tip radius of 50 nm. The resist's relative dielectric constant was 3. The tip-substrate bias voltage was -82 V, the resist thickness was 100 nm, and a 10-nm-deep tip indentation into the resist surface was assumed. Figure 4 shows the calculated electric flux lines with the contour lines of the electric field inside the resist.

We next discuss the mechanism of the latent-image formation inside the resist when using our exposure system. A mechanism of exposure using STM lithography was simulated in Dobisz et al.[9] In this analysis, the electrons were field-emitted from the tip and most of the energy from the bias voltage was given to the electrons before they reached

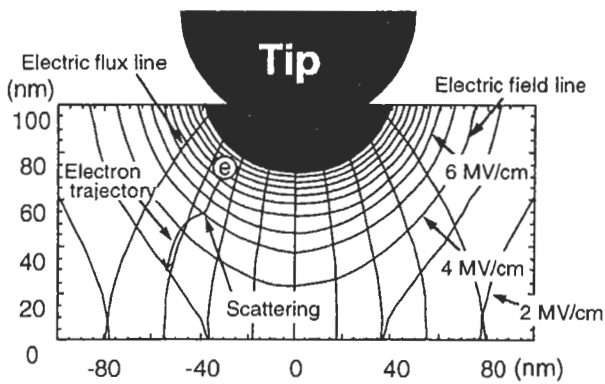


Fig.4 Calculated electric flux lines and contour lines of the electric field inside the resist.

the resist surface. Thus, the exposure mechanism using the electron is similar to that for EB lithography, except for the low energy of the electrons. However, the mechanism of our proposed AFM lithography differs from their STM lithography. In our method, the tip makes contact and indents the surface of the resist, but in STM lithography the tip does not touch the resist surface.

Based on our analysis of the resist shape and the mapping of the electric field, the mechanism of AFM lithography can be explained as follows. Electrons, which are field-emitted from the tip into the resist, travel mainly along the electric flux lines while gaining energy from the electric field. If an electron obtains enough energy to cause a chemical reaction with a molecule of the resist, it reacts with the resist with a certain probability. To form a latent image in the resist from electrons, the number of chemical reactions per unit volume of the resist must exceed some critical value determined by the resist material. Therefore, the latent image is formed along the lines of electric flux at a large exposure, and thus the trapezoidal shape of the developed resist is explained by the shape of the electric flux lines. At a small exposure, however, only a few electrons have enough energy to cause a chemical reaction and the number of chemical reactions per unit volume of the resist may not exceed the critical value. This is more significant near the substrate because the electric flux lines diverge there. Thus, the upside-down trapezoidal latent image is obtained.

We have also examined the dependence of the pattern linewidth on the exposure for each of the resist thicknesses. The linewidths of the pattern decrease as the exposure dose decreases, but this dependence (dose-margin)

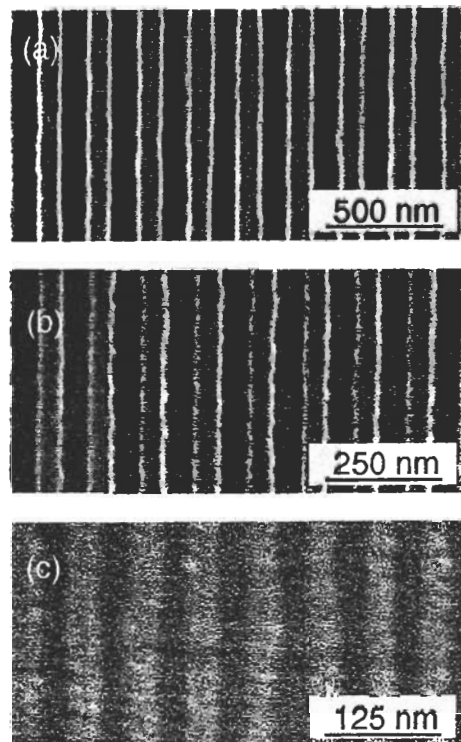


Fig.5 SEM top views of the line-and-space resist patterns showing the minimum line width for resist thicknesses of (a) 100, (b) 40, and (c) 15 nm.

becomes weaker as the resist thickness decreases. Furthermore, the resolution depends on the resist thickness. It may also be possible to explain these relationships in terms of the current distribution inside the resist and the indentation of the tip into the resist. However, we need to investigate this possibility further in order to discuss it more quantitatively. The SEM image of the minimum line width we obtained is shown in Fig. 5. For the resist thicknesses of 15, 40, and 100 nm, the minimum linewidths we obtained were respectively 27, 55, and 110 nm.

Figure 6 (a) shows an SEM micrograph of the pattern for the case of the 40-nm-thick resist, and Fig. 6 (b) shows the scanning trajectory of the tip and expected patterns using different proximity effect amounts. The scanning pitch was 50 nm and the line width was 60 nm. The proximity effect is one of the major factors limiting the resolution of EB lithography. If a sharp-corner pattern is exposed by EB lithography without dose correction, the corner's shape is deformed as in Fig. 6 (b). However, Fig. 6 (a) shows that the deviation of the pattern shape from the ideal pattern is less than 5 nm, which is clearly one of the advantages of AFM lithography over EB

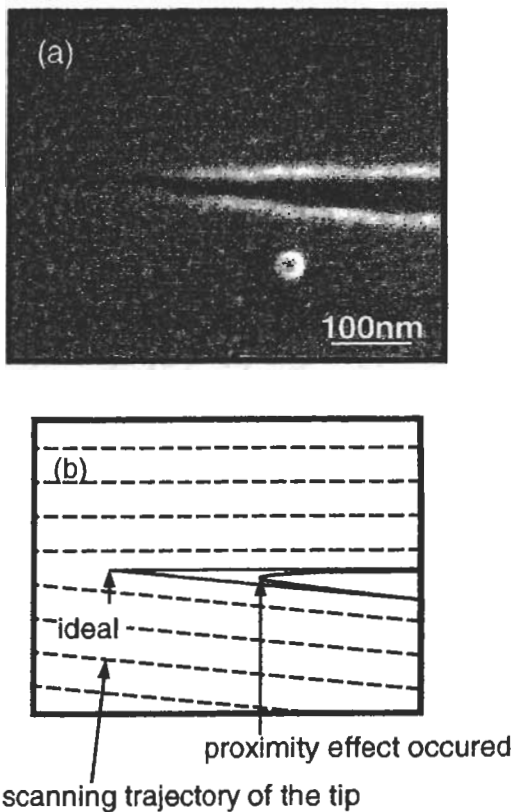


Fig.6 (a) SEM micrograph of a resist pattern with a sharp corner. (b) The scanning tip trajectory (dotted line) and expected pattern deformation using single Gaussian for the energy distribution.

lithography. The proximity effect is small because the scattered electrons have little energy (momentum) and they are also accelerated along the electric flux lines.

In conclusion, we fabricated a line-and-space pattern on a negative resist and investigated the characteristics of nanolithography using AFM with a current-controlled exposure system. Although the sensitivity depended on the thickness of the resist, the electric field strength for each sensitivity point was constant. For the resist thicknesses of 15, 40, and 100 nm, we obtained minimum resist-line widths of 27, 55, and 110 nm, respectively. The cross-sectional shape of the pattern was trapezoidal at a higher exposure dose and upside-down trapezoidal at a lower exposure dose. We evaluated the electric-field mapping inside the resist and explained the characteristics of the AFM exposure system based on the proposed exposure mechanism. The advantage, in terms of the proximity effect, of AFM lithography over EB and STM lithography was discussed.

Reference

1. M. A. McCord and R. F. W. Pease, *J. Vac. Sci. Technol.* B4, **86** (1986).
2. E. A. Doboisz, and C. R. K. Marrian, *Appl. Phys. Lett.* **58**, 2526 (1991).
3. C. R. K. Marrian, E. A. Doboisz, and J. A. Dagata, *J. Vac. Sci. Technol.* B10, 2877 (1992).
4. A. Majumdar, P. I. Oden, J. P. Carrejo, L. A. Nagahara, J. J. Graham, and J. Alexander, *Appl. Phys. Lett.* **61**, 2293 (1992).
5. E. S. Snow, and P. M. Campbell, *Appl. Phys. Lett.* **64**, 1932 (1994).
6. K. Kragler, E. Gunther, R. Leuschner, G. Falk, A. Hammerschmidt, H. Vonseggem, and G. Saemannschenko, *Appl. Phys. Lett.* **67**, 1163 (1995).
7. S. W. Park, H. T. Soh, C. F. Quate, and S. -I. Park, *Appl. Phys. Lett.* **67**, 2415 (1995).
8. H. T. Soh, K. Wilder, A. Atalar, and C. F. Quate, *Digest of Technical Papers, 1997 Symposium on VLSI Technology* 129 (1997); K. Wilder, H. T. Soh, A. Atalar, and C. F. Quate, *J. Vac. Sci. Technol.* B15, 1811 (1997).
9. E. A. Doboisz, H. W. P. Koops, and F. K. Perkins, *Appl. Phys. Lett.* **68**, 3653 (1996).